journal

J. Am. Ceram. Soc., **80** [11] 2828–36 (1997)

In-Situ Transmission Electron Microscopy Crystallization Studies of Sol–Gel-Derived Barium Titanate Thin Films

Maria C. Gust,*,† Neal D. Evans,‡ Leslie A. Momoda,*,§ and Martha L. Mecartney*,†

Department of Chemical and Biochemical Engineering, University of California, Irvine, California 92697-2575, Oak Ridge Institute for Science and Education, Oak Ridge, Tennessee 37831-0117, and Hughes Research Laboratories, Malibu, California 90265

Barium titanate ($BaTiO_3$) thin films that were derived from methoxypropoxide precursors were deposited onto (100) Si, Pt/Ti/SiO_2/(100) Si, and molecular-beam-epitaxy-grown (MBE-grown) (100) $BaTiO_3$ on (100) Si substrates by spin coating. The crystallization behavior of the amorphous-gel films was characterized using *in-situ* transmission electron microscopy heating experiments, glancing-angle X-ray diffraction, and differential thermal analysis/thermogravimetric analysis. Amorphous-gel films crystallized at a temperature of ~600°C to an intermediate nanoscale (5–10 nm) barium titanium carbonate phase, presumably $BaTiO_2CO_3$, that subsequently transformed to nanocrystalline (20–60 nm) $BaTiO_3$. Random nucleation in the bulk of the gel film was observed on all substrates. In addition, oriented growth of $BaTiO_3$ was concurrently observed on MBE-grown $BaTiO_3$ on (100) Si. High-temperature decomposition of the intermediate carbonate phase contributed to nanometer-scale residual porosity in the films. High concentrations of water of hydrolysis inhibited the formation of the intermediate carbonate phase; however, these sols precipitated and were not suitable for spin coating.

I. Introduction

BARIUM TITANATE ($BaTiO_3$) is an attractive material for applications such as multilayer capacitors, pyroelectric detectors, ferroelectric memory, and positive temperature coefficient (PTC) sensors. In thin-film form, the material has the potential to be integrated directly into microelectronic devices. $BaTiO_3$ thin films have been fabricated using various methods, including metal–organic chemical vapor deposition (MOCVD),[1–3] radio-frequency (rf) sputtering,[4–6] evaporation,[7] molecular beam epitaxy (MBE),[8] and laser ablation.[9–11] Wet chemical methods, such as sol–gel[12–18] and metal–organic decomposition (MOD),[19–21] also have been successfully used in the preparation of $BaTiO_3$ thin films. One of the biggest advantages wet chemical methods have over other deposition techniques is that the experimental setup that is required is relatively inexpensive, because no high-vacuum system is needed. The wet chemical methods also offer the potential for improved compositional control and homogeneity.

Relatively fine-grained microstructures with grain diameters of <70 nm have been commonly observed in polycrystalline $BaTiO_3$ thin films.[4,9,15,22–25] The predominantly reported crystal structure of $BaTiO_3$ thin films with nanometer-sized grains is the cubic perovskite structure at room temperature, rather than the equilibrium ferroelectric tetragonal structure.[4,26] The electrical properties of bulk $BaTiO_3$ are known to be dependent on the grain size, with a decreasing dielectric constant with decreasing grain size below a critical value.[27] If similar behavior is assumed for thin films, films with nanometer-sized grains may not have optimal dielectric properties. Evidence for a grain-size dependence on the dielectric properties has been observed in sol–gel-[15] and MOD-derived[19] $BaTiO_3$ thin films, where the value of the dielectric constant decreased as the grain size decreased. Consequently, a better understanding of the nucleation and grain-growth behavior of these films should aid in improving film microstructure and properties.

Interfacial reactions between the film and substrate materials is another concern when growing $BaTiO_3$ thin films. This interface can have a detrimental effect on the properties of the thin-film/substrate material, such as a decrease in dielectric constant due to the formation of low-dielectric material at the interface.[5] As a result, it is critical to be able to control the reactions that occur at the interface, to optimize the electrical performance of the material.

In this work, the crystallization of sol–gel-derived $BaTiO_3$ thin films on various substrates was studied, to characterize the crystallization sequence, the interface between the film and substrate, and the role that the lattice-parameter match of the substrate might have in influencing nucleation. The primary tool that was used in this investigation was transmission electron microscopy (TEM), which included *in-situ* heating that allowed the crystallization behavior of amorphous-gel films to be observed directly.

II. Experimental Procedure

The sol was prepared by dissolving a commercially available Ba-Ti methoxypropoxide (Gelest, Tullytown, PA) in methoxypropanol in a dry-nitrogen glove box and refluxing the solution for ~12 h. This alkoxide precursor is significantly less of a health hazard than the more-commonly used methoxyethoxide precursors. The final sol concentration was 0.25*M* of Ba-Ti, with no deliberately added water of hydrolysis. Some water of hydrolysis was inadvertently introduced during film preparation from moisture in the air. When higher water concentrations were intentionally used (>1 mol water/mol alkoxide), precipitates formed within minutes in the sols that had been refluxed; therefore, films could not easily be fabricated.

Thin films were fabricated on (100) Si, sputter-deposited Pt/Ti/SiO_2/(100) Si, and MBE-grown $BaTiO_3$ on (100) Si substrates by spin coating the sol at 2000 rpm for 1 min in air. (See McKee *et al.*[8] for experimental details on the preparation of the MBE-grown $BaTiO_3$.) After deposition of each layer, films were given a pyrolysis heat treatment on a hot plate at 350°C for 5 min to remove residual organics. Five layers were deposited onto each substrate, for a total film thickness of ~300 nm.

C. Randall—contributing editor

Manuscript No. 191410. Received November 4, 1996; approved March 28, 1997.
Supported by the following: Hughes Research Laboratories, in conjunction with the State of California MICRO Program; the Division of Materials Science, U.S. Department of Energy, under Contract No. DE-AC05-96OR22464 with Lockheed Martin Energy Research Corporation; and the SHaRE Program, under Contract No. DE-AC05-76OR00033 with Oak Ridge Associated Universities.

*Member, American Ceramic Society.
†Department of Chemical and Biochemical Engineering.
‡Oak Ridge Institute for Science and Education.
§Hughes Research Laboratories.

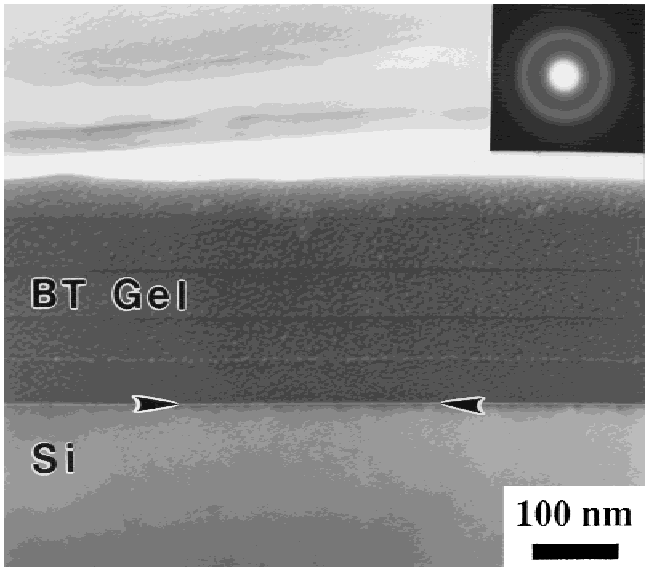

Fig. 1. Cross-sectional bright-field TEM micrograph and corresponding electron diffraction pattern (inset) of amorphous pyrolyzed Ba-Ti methoxypropoxide gel film on (100) Si. Arrows indicate oxidized silicon interfacial layer.

Pyrolyzed films were either crystallized by annealing at 750°C for 1 h in an oxygen atmosphere or made directly into thin foils for *in-situ* TEM studies.

The crystallization behavior of the heat-treated films was studied using glancing-angle X-ray diffraction (XRD) (Model D5000 Diffractometer, Siemens, Karlsruhe, Germany), with incident rays at an angle of 2° to the film surface. Microstructural characterization of the crystalline $BaTiO_3$ films was performed using an analytical TEM microscope (Model CM20, Philips, Eindhoven, The Netherlands) at a voltage of 200 kV. Samples were prepared for TEM using conventional dimpling and ion-milling procedures.

For the *in-situ* TEM studies, thin TEM foils of pyrolyzed films were prepared by dimpling and ion milling. Planar-view and cross-sectional samples both were made. The *in-situ* hot-stage experiments were conducted using an instrument (Model CM30, Philips) that was operated at 300 kV and a single-tilt heating holder (Model 628, Gatan, Pleasanton, CA). The samples were initially heated to 300°C in the microscope and held at this temperature for ~5 min to burn off water and contaminants. Following this, the samples were heated to the desired temperature within a couple of minutes. The accuracy of the temperature measurement was dependent on the thermal contact between the sample and the stage, and it is estimated that these experiments may have had temperature deviations of up to 100°C lower than the measured temperatures. Prior XRD studies indicated that films that were heat treated in a vacuum furnace formed $BaTiO_3$ at the same temperatures as films that were heat treated in air; therefore, it was assumed that the vacuum of the microscope should not inhibit crystallization. The *in-situ* experiments may not be fully representative of normal processing conditions, because of the extremely low partial pressure of oxygen in the microscope. (However, the authors note that the microstructures of samples that were annealed in and outside the TEM microscope were strikingly similar.) Regions to be photographed were removed from the electron beam whenever possible, to minimize dose-related effects from the 300 keV electrons.

Thermochemical properties of dried-gel powders were determined using differential thermal analysis (DTA) and thermogravimetric analysis (TGA) (Model 2100 Thermal Analysis System, duPont, Wilmington, DE). Sols were dried in a vacuum furnace at 100°C and gently crushed to fine powder using a mortar and pestle. The dried powders were heated in air to 1000°C at a ramp rate of 10°C/min.

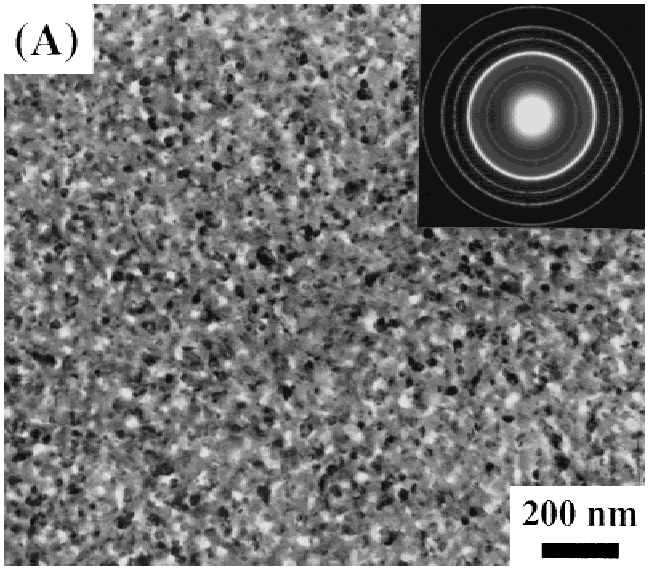

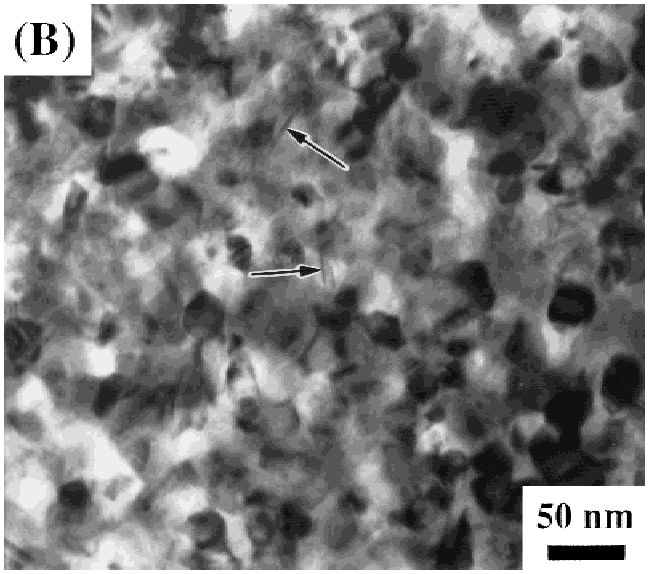

Fig. 2. Crystallized $BaTiO_3$ on (100) Si ((A) planar view (with corresponding electron diffraction pattern in inset) and (B) higher magnification of film showing presence of twins in some grains, as indicated by arrows).

III. Results

(1) Analysis of Ex-situ Crystallized $BaTiO_3$ Films

A TEM micrograph of a cross section of the pyrolyzed gel film on (100) Si is shown in Fig. 1. All TEM images are bright-field images, using the transmitted beam to form the image, unless otherwise noted. The diffuse halo in the inset electron diffraction pattern indicates that the film is amorphous. Each of the five layers is ~60 nm thick and contains residual porosity. The nonuniformity of the top layer is due to ion milling during TEM sample preparation. A distinct, thin amorphous layer with a thickness of 5–10 nm is present along the interface between the substrate and the film. This layer, with lower electron scattering, has been analyzed by Auger depth profiling and is associated with oxidized silicon.

Figure 2(A) shows a TEM micrograph of a planar-view sample and the corresponding electron diffraction pattern of a $BaTiO_3$ film that has been deposited on (100) Si and heat treated at 750°C for 1 h in oxygen *ex situ.* The film consists of randomly oriented equiaxed grains that are 20–60 nm in diam-

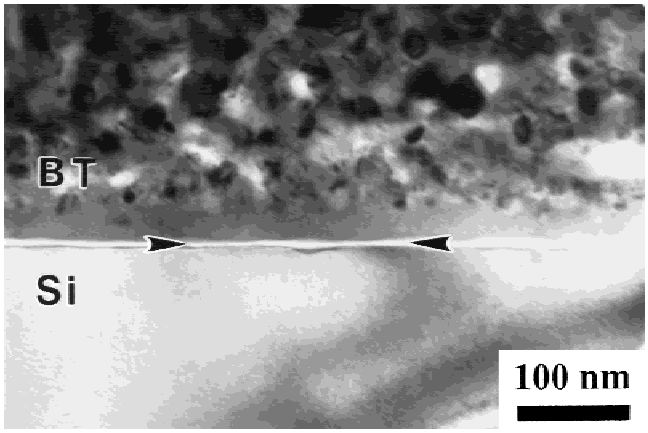

Fig. 3. Cross-sectional TEM micrograph of crystallized $BaTiO_3$ film on (100) Si; heat treatment of 750°C for 1 h has been applied. Arrows indicate oxidized silicon interfacial layer; a residual amorphous region in the film can be observed near the oxidized silicon layer.

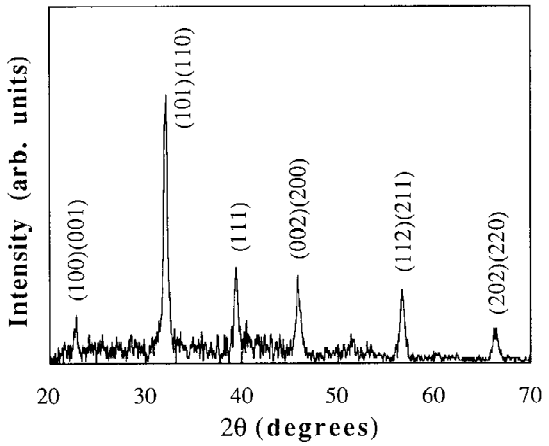

Fig. 4. Glancing-angle thin-film XRD pattern of $BaTiO_3$ film on (100) Si.

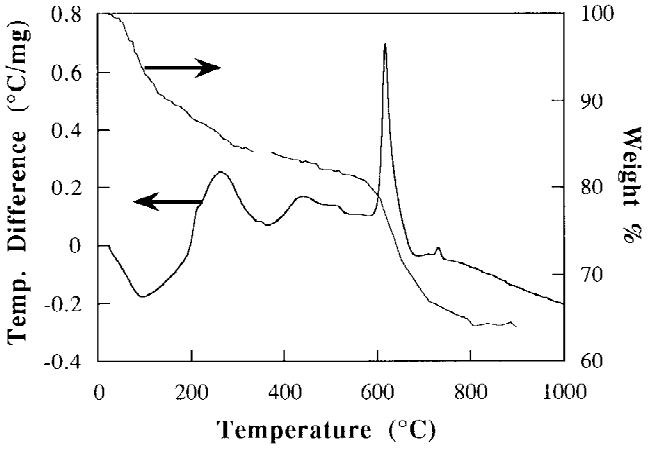

Fig. 5. DTA/TGA of Ba-Ti methoxypropoxide dried-gel powders.

eter. No ferroelectric domains are observed. Twins are observed in some grains (Fig. 2(B)). The film also contains residual porosity, with a pore size on the order of the grain size. The electron diffraction pattern is consistent with perovskite $BaTiO_3$, with trace amounts of a second phase at *d*-spacings of 3.32 and 2.61 Å.

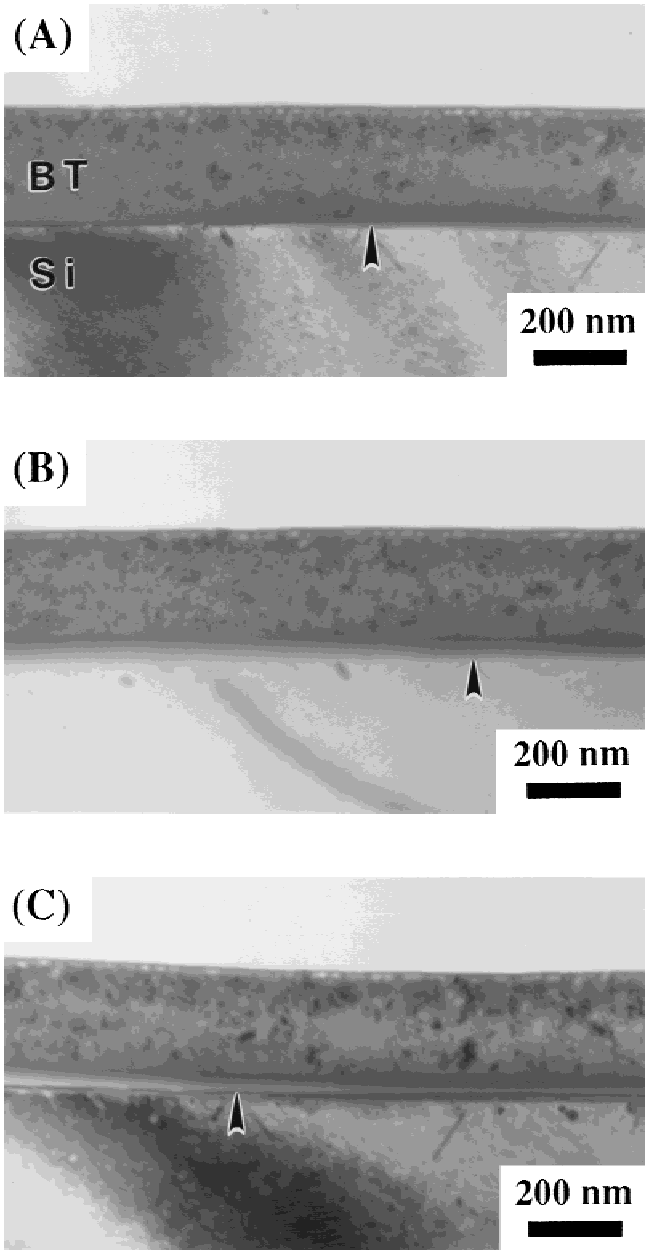

Fig. 6. Cross-sectional TEM micrographs of $BaTiO_3$ film on (100) Si after *in-situ* TEM heating at 750°C for (A) 0.5, (B) 5, and (C) 8 h. Arrows indicate same region of film.

A cross-sectional TEM micrograph (Fig. 3) of the heat-treated film on (100) Si again shows an amorphous layer along the film/substrate interface. Despite the heat treatment at 750°C for 1 h, the thickness of the oxidized silicon layer did not change significantly and remained <10 nm. The film was polycrystalline, except for the regions near the substrate. Regions of the film up to 20–40 nm away from the interface were amorphous. There was significant inward diffusion of silicon in these regions, as determined by Auger electron spectroscopy (AES) and nanoprobe energy-dispersive X-ray spectroscopy (EDS) studies. Compositional analyses and electron diffraction suggest that this is an amorphous barium titanium silicate phase.

The XRD pattern of the $BaTiO_3$ film in Figs. 2 and 3 is shown in Fig. 4. All the diffraction peaks correspond to $BaTiO_3$. Unlike the electron diffraction pattern in Fig. 2(A), the XRD pattern does not show any evidence of any second phases; therefore, the second phase that is found by TEM diffraction must be present in trace amounts. No peak splitting is

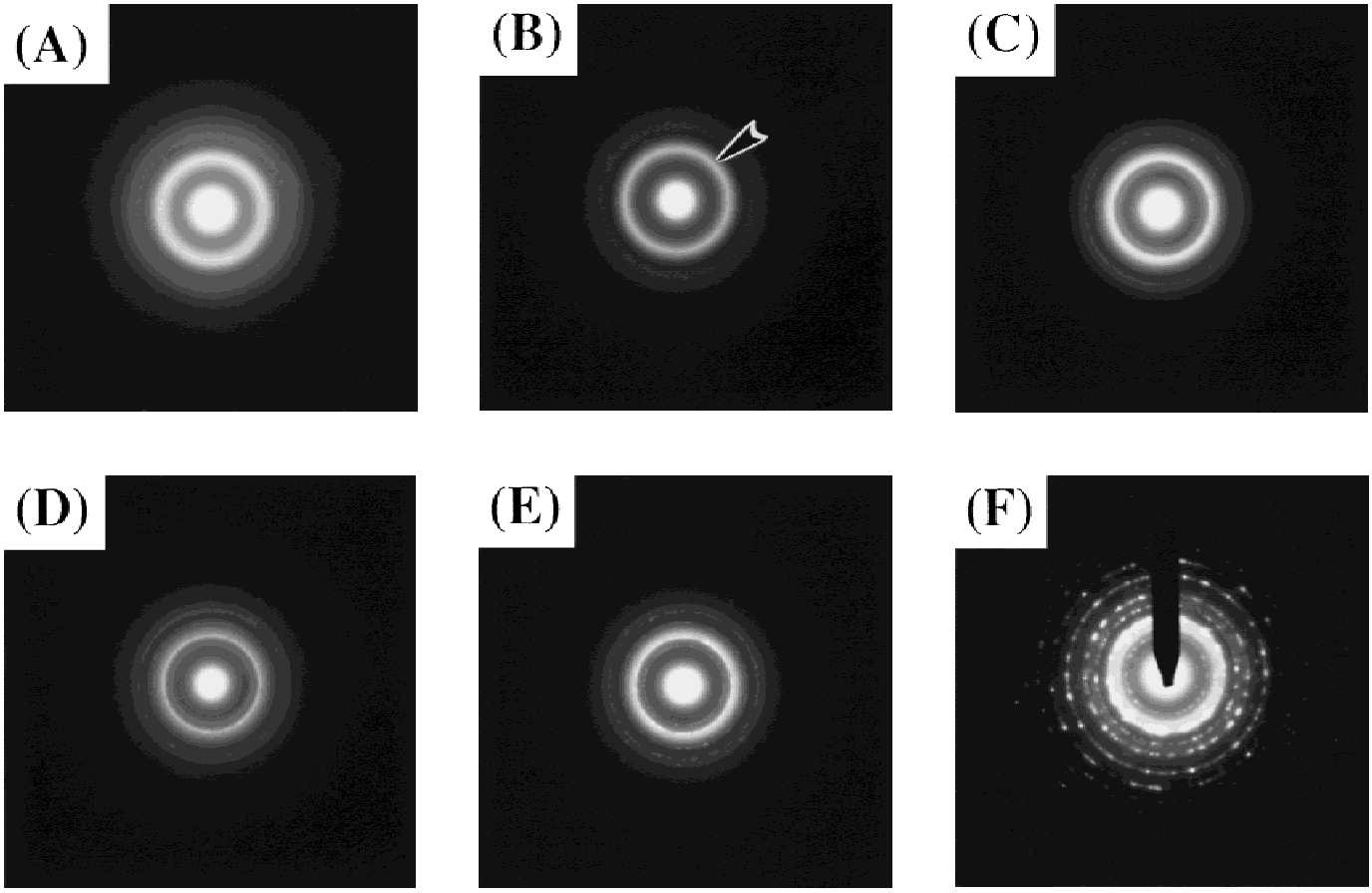

Fig. 7. Electron diffraction patterns of $BaTiO_3$ film on (100) Si after *in-situ* TEM heating at 750°C for (A) 0 min, (B) 10 min, (C) 20 min, (D) 2.5 h, (E) 2.5 h + 0.5 h at 800°C, and (F) 2.5 h + 1 h at 800°C. Arrow indicates diffraction ring due to intermediate phase at $d = 3.32$ Å.

observed between the (101) and (110) or higher-order planes, although with such a fine grain size, this would be difficult to identify clearly. This observation, in addition to the absence of ferroelectric domain images by TEM, suggests that the material may not be ferroelectric and tetragonal but rather primarily cubic. (Thin-film samples also did not show ferroelectric hysterisis loops of applied field versus polarization when measured for ferroelectric behavior.)

Figure 5 shows the DTA and TGA results of the dried-gel powders. The endothermic and exothermic peaks and gradual weight loss at temperatures <600°C are due to the removal of organics in the system. There is a large exothermic reaction at ~620°C, as indicated by the large peak in the DTA plot. As shown by TGA, this reaction is associated with a weight loss of 16%, which is indicative of a decomposition reaction. There also is a small exothermic peak with no associated weight loss at ~735°C.

(2) In-Situ Characterization

The evolution of the film microstructure at 750°C using *in-situ* TEM is shown in Fig. 6. Cross-sectional TEM micrographs of the film on (100) Si show that the film has begun to crystallize after 30 min at 750°C (Fig. 6(A)). The highest concentration of nucleating sites was noted at the free surface of the film and at the interfaces between each of the five deposited layers. Crystallization was further enhanced with time; however, even after 8 h at 750°C (Fig. 6(C)), the film was not entirely crystalline. The film region near the substrate remained amorphous. This region had a thickness of ~20–40 nm, which is similar to the *ex-situ* heat-treated film (Fig. 3). The inward diffusion of silicon may have a similar role here, with the subsequent stabilization of an amorphous phase.

Figure 7 shows a crystallization time sequence of the film at 750°C using *in-situ* TEM diffraction patterns with a selected area of several micrometers. The film begins amorphous (Fig. 7(A)) and starts to crystallize after 10 min (Fig. 7(B)) and, after 20 min at 750°C, clearly shows polycrystalline diffraction rings of $BaTiO_3$ (Fig. 7(C)). However, initial crystallization at 10 min shows a bright diffraction ring at $d = 3.32$ Å, which cannot be due to $BaTiO_3$. At longer times (and a higher temperature of 800°C, to enhance diffusion and accelerate the reaction), the intensity of this ring due to the intermediate phase decreases and the $BaTiO_3$ diffraction rings become less continuous, which indicates grain growth of $BaTiO_3$. Finally, in Fig. 7(F), the film is polycrystalline $BaTiO_3$ with only traces of the second phase. (Note that the temperatures that are given here are only approximate, because the exact temperature of any particular region of the film is not measured—only the temperature of the heating sample holder.)

Films were deposited onto (100) Si with a platinum barrier layer, to avoid forming the residual amorphous-silicon-rich layer in the $BaTiO_3$ film. A pyrolyzed gel film on Pt/Ti/SiO_2/(100) Si is shown in Fig. 8. The gel film was amorphous and had a uniform thickness of ~300 nm. The (111) oriented polycrystalline platinum layer had a rough surface, as did the titanium layer, with a roughness on the order of 5–10 nm. The microstructural evolution of the film on platinum during *in-situ* heating at 700°C is shown in Fig. 9. The lower temperature of 700°C was selected to capture the crystallization events on film more easily. Similar to the gel film on (100) Si, the film first crystallized to an intermediate phase and then transformed to $BaTiO_3$ with trace amounts of the second phase. However, rather than the nucleation occurring randomly in the bulk of the gel film, nucleation was concentrated near the film/platinum

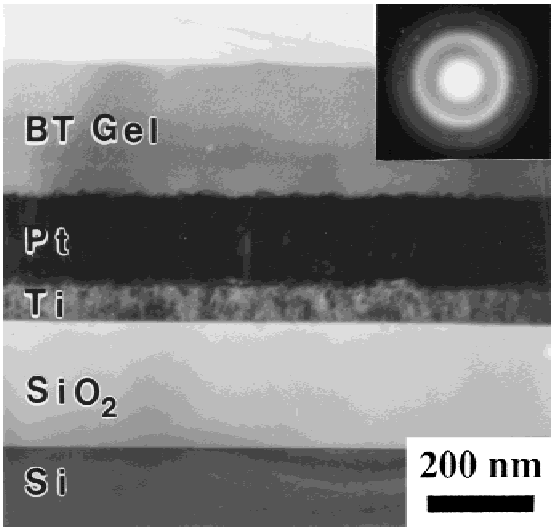

Fig. 8. Cross-sectional TEM micrograph of amorphous pyrolyzed Ba-Ti methoxypropoxide gel film on Pt/Ti/SiO_2/(100) Si; the corresponding electron diffraction pattern is shown in the inset.

interface. Radiation damage prevented complete crystallization of the gel film for this sample. (There also was damage to the substrate layers, with holes forming in the platinum and degradation of the uniformity of the titanium layer.)

A sol–gel film was deposited onto MBE-grown $BaTiO_3$ on (100) Si, to provide an ideal template for nucleating $BaTiO_3$ and to inhibit the formation of the intermediate phase. Figure 10 shows a cross section of the heterostructure and the corresponding electron diffraction patterns for the different layers with a pyrolyzed gel film. In Fig. 10(A), the MBE-grown $BaTiO_3$ is shown to be very dense and has a uniform thickness of ~100 nm, on the scale that was observed by TEM. In the diffraction patterns, the gel film also is shown to be amorphous (Fig. 10(C)) and the $BaTiO_3$ is (100) oriented with the (100) Si (Fig. 10(F)).

The gel film remained amorphous at temperatures <600°C. Figure 11 shows the film after 25 min at 600°C, where the gel film has begun to crystallize to the intermediate phase. There is no nucleation observed along the interface. The intermediate phase, as indicated by the white spots in the dark-field micrograph, has a grain size of 5–10 nm and is randomly distributed throughout the film. The same type of crystallization behavior is observed in a gel film that has been heated to 650°C for 20 min.

Figure 12 shows the *in-situ* TEM results for the film that was held at 700°C for 0.5, 1, and 1.5 h. At this temperature, there was evidence of oriented $BaTiO_3$ growing on the MBE-grown $BaTiO_3$. However, concurrent random nucleation of $BaTiO_3$ in the bulk of the gel film also was observed.

Figure 13 shows the film on MBE-grown $BaTiO_3$ after holding for 5.5 h at 700°C. Even after holding for long times, the diffraction pattern shows some polycrystalline randomly oriented $BaTiO_3$, in addition to the oriented $BaTiO_3$ near the interface.

IV. Discussion

The nanocrystalline (20–60 nm) and nanoporous microstructure of these films is typical for $BaTiO_3$ films that have been prepared using methoxypropoxide-based sols.[24] This microstructure has been observed to form in this system relatively independent of variations in processing parameters such as water of hydrolysis (for $h < 2$, where h is the number of moles of water per mole of alkoxide), heat treatment, or type of substrate.[24] A similar microstructure also has been observed in films that have been prepared using an ethoxide-based sol with diethylamine and acetylacetone additives.[28] A similar

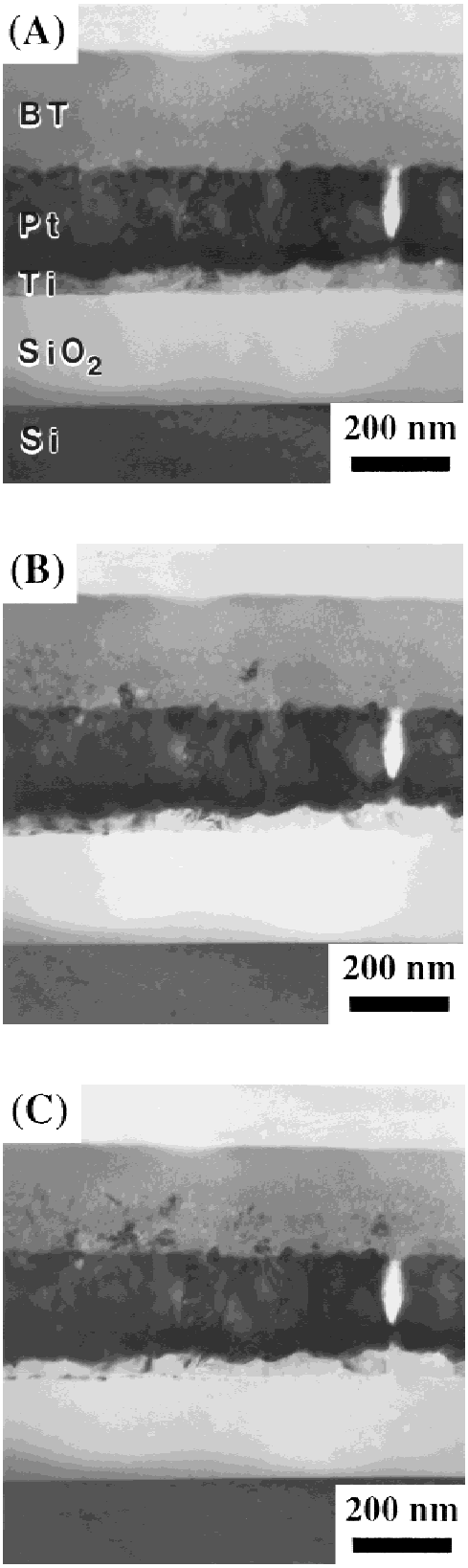

Fig. 9. Cross-sectional TEM micrographs of $BaTiO_3$ film on Pt/Ti/SiO_2/(100) Si after *in-situ* TEM heating at 700°C for (A) 20 min, (B) 1 h, and (C) 2 h. Note the increased nucleation density near the film/platinum interface, compared to that of the film on silicon (Fig. 6).

nanocrystalline microstructure, with a grain size of 25–50 nm, was observed by Xu *et al.*,[15] using a methoxyethoxide-based sol. Kumar and Messing[23] observed grains <60 nm in size in a Pechini-process-derived $BaTiO_3$ film, where the precursor that

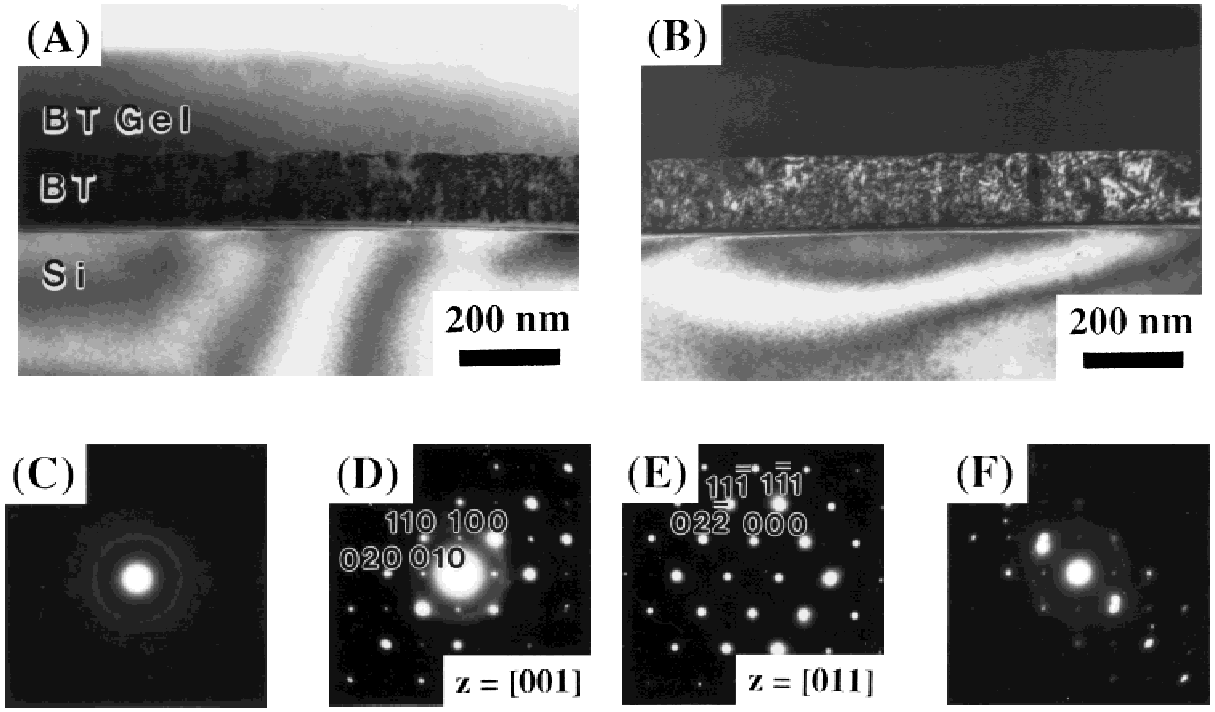

Fig. 10. Cross-sectional TEM micrographs ((A) bright field and (B) dark field, using the (110) MBE-grown $BaTiO_3$ reflection and the $(11\bar{1})$ Si reflection) and corresponding electron diffraction patterns of amorphous pyrolyzed $BaTiO_3$ gel film on (100) $BaTiO_3$/(100) Si ((C) gel film, (D) (100) $BaTiO_3$, (E) (100) Si, and (F) $BaTiO_3$ and (100) Si).

was used was $BaCO_3$ that had been dissolved in a titanium solution that consisted of tetraisopropyl titanate, ethylene glycol, and citric acid.

A key to understanding the fine-grained microstructure of these materials lies in understanding their nucleation behavior. There is debate over the crystallization path of $BaTiO_3$ that is derived from wet chemical methods. One possibility is that $BaTiO_3$ forms via a solid-state reaction between $BaCO_3$ and anatase TiO_2; this has been suggested for neodecanoate-based[29] and acetate-based[30] precursors, where the reaction temperatures were in the range of 600°–650°C. Another possibility is the formation of $BaTiO_3$ via the crystallization and transformation of an intermediate oxycarbonate phase. This type of reaction has been observed for powders that have been formed using oxalates,[31] citrates,[32] metal–organic resin,[33] and methoxyethoxide[34] precursors.

In this work, the amorphous gel film crystallized at a temperature of ~600°C (Fig. 11). At the onset of crystallization, the most-intense electron diffraction ring had a *d*-spacing of 3.32 Å. This *d*-spacing does not match $BaTiO_3$, $BaCO_3$, or anatase TiO_2, although the 100% intensity peak of rutile TiO_2 has a *d*-spacing of 3.25 Å[35] and was considered to be a possible intermediate phase.[28] Barium silicate (which is isostructural with barium strontium silicate, $BaSrSi_2O_6$[36]) was another possibility that was considered;[24] however, the intermediate phase formed even in the absence of silicon. The *d*-spacing also does not match other barium titanium oxides, such as Ba_2TiO_4, $BaTi_2O_5$, $BaTi_3O_7$, or $BaTi_4O_9$, that have been observed in $BaTiO_3$ that has been derived from ethoxide precursors.[13,17] However, the most-intense diffraction ring at 3.32 Å and a less-intense ring at 2.62 Å from the selected-area diffraction patterns are *d*-spacings that are consistent with those that were observed by Kumar *et al.*[33] and Frey and Payne[34] in XRD analysis of dried powders from the Pechini process and methoxyethoxide sols. Based on DTA/TGA results, Raman spectroscopy, and Fourier transform infrared spectroscopy, these researchers have suggested that this phase is a carbonate with a stoichiometry that is close to $Ba_2Ti_2O_5CO_3$.[31,33,34] The limited diffraction information that is available (two *d*-spacings) precludes crystal structure analysis of this phase.

The formation and decomposition of this intermediate phase can be observed in the DTA/TGA results of methoxypropoxide-derived $BaTiO_3$ powders (Fig. 5). The large exothermic peak at 620°C is consistent with the temperature at which crystallization of the intermediate phase is first observed by *in-situ* TEM. A lower temperature of crystallization of the intermediate phase for the *in-situ* experiments may be due to the crystallization of films rather than dried-gel powders. The weight loss that is associated with the exothermic peak indicates that this phase is unstable at these temperatures, because it decomposes almost immediately after it forms; this also is indicated by TEM, because the intensity of the diffraction ring at 3.32 Å decreases as the diffraction rings for $BaTiO_3$ increase in intensity when samples are held at a temperature of 700°C.

The theoretical weight loss for the transformation of $Ba_2Ti_2O_5CO_3$ to $BaTiO_3$ is 8.6%. This weight loss (in the temperature range of 600°–700°C) was measured in experiments by Kumar *et al.*[33] in metal–organic-resin-derived $BaTiO_3$. However, Frey and Payne[34] observed a weight loss of ~15% in the temperature range of 600°–700°C in a methoxyethoxide-based sol. Both research groups observed similar XRD peaks of dried powders for the intermediate phase and attributed them to $Ba_2Ti_2O_5CO_3$. However, the weight loss of ~20% that is associated with the exothermic reaction in the DTA/TGA data in Fig. 5 is more consistent with the decomposition of $BaTiO_2CO_3$ (calculated to be 16%). (Note that this is the same weight loss that would be present for a solid-state reaction between $BaCO_3$ and TiO_2 to form $BaTiO_3$; however, because *d*-spacings that matched $BaCO_3$ or TiO_2 were never observed during *in-situ* TEM heating, the crystallization of $BaTiO_3$ is believed to be via the transformation of an intermediate $BaTiO_2CO_3$ phase.)

There is a large driving force for the nucleation of the intermediate carbonate phase. Some preferential nucleation and growth of $BaTiO_3$ has been observed at the platinum/gel interface, because of the close lattice match (~3%) between platinum and cubic $BaTiO_3$; however, a high degree of random nucleation in the bulk of these films also has occurred (Fig. 9). Even when the sols are spun coated onto $BaTiO_3$ substrates, homogeneous nucleation of the carbonate phase is observed in

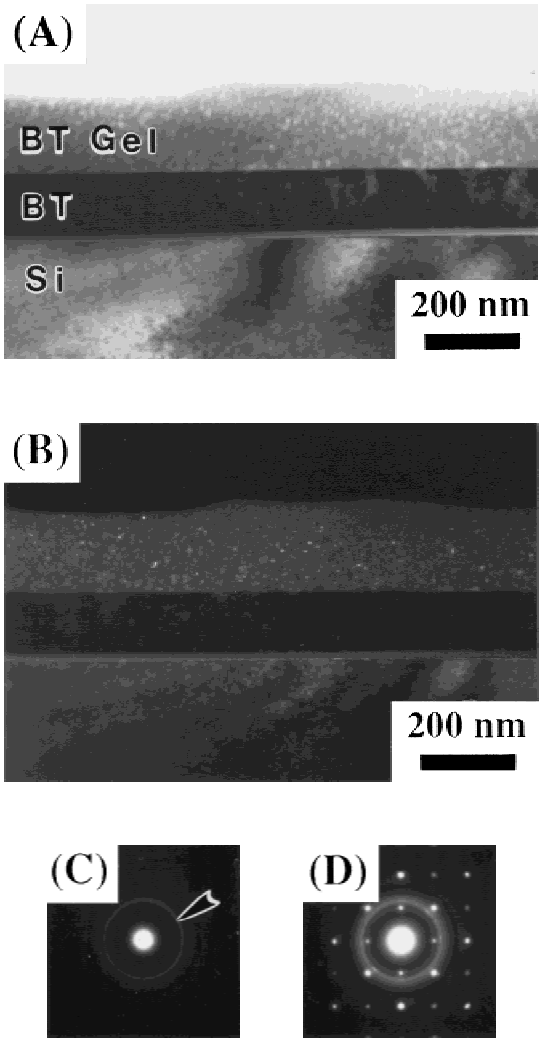

Fig. 11. Cross-sectional TEM micrographs ((A) bright field and (B) dark field, using the diffuse ring in the diffraction pattern) and corresponding electron diffraction patterns of sol–gel $BaTiO_3$ gel film on $BaTiO_3$/(100) Si after *in-situ* TEM heating at 600°C for 25 min ((C) gel film and (D) gel film, $BaTiO_3$, and (100) Si), showing nucleation of the intermediate phase with $d = 3.32$ Å (indicated by the arrow).

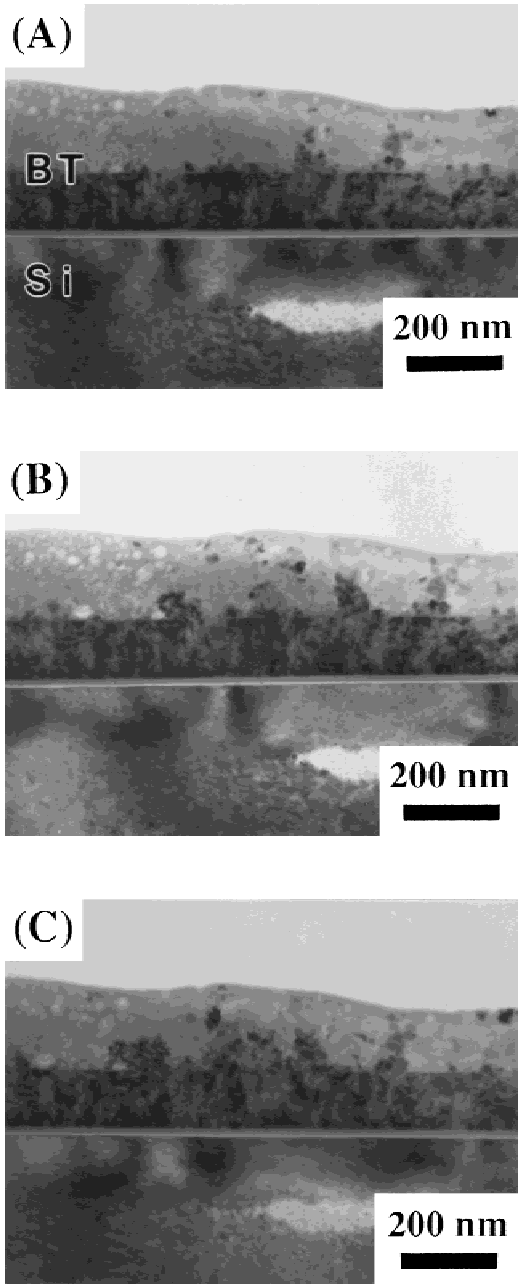

Fig. 12. Cross-sectional TEM micrographs of sol–gel $BaTiO_3$ film on $BaTiO_3$/(100) Si after *in-situ* TEM heating at 700°C for (A) 0.5, (B) 1, and (C) 1.5 h. Note the crystallization of $BaTiO_3$ at the gel/$BaTiO_3$ interface and in the bulk of the gel film.

the bulk of the gel film, which competes with nucleation of $BaTiO_3$ at the interface and oriented growth (Fig. 12). The high nucleation density of the intermediate phase, which transforms to $BaTiO_3$, results in the formation of fine-grained polycrystalline $BaTiO_3$. Similar microstructures have been observed by the authors for *ex-situ* annealed films,[24] which indicates that random nucleation dominates, irrespective of the high surface area of the TEM samples.

Rapid formation of $BaTiO_3$ grains also may be the cause of the twins that have been observed by TEM (Fig. 2(B)). Growth twins have been observed in other $BaTiO_3$ thin-film microstructures.[9,15,23] These {111} growth twins also have been found to be due to anomalous grain growth below the eutectic temperature in bulk $BaTiO_3$.[37]

Residual porosity in the crystallized films may be attributed, in part, to organic decomposition at high temperatures. The DTA/TGA studies of the dried-gel powders indicate that the intermediate phase crystallizes at a temperature of ~620°C and $BaTiO_3$ crystallizes at a temperature of ~735°C (Fig. 5). If similar thermochemical properties are assumed for thin films, the kinetics of densification may not be fast enough after the high-temperature decomposition of the carbonate intermediate for the film to densify prior to the onset of crystallization. The residual porosity also may be a consequence of rigidity in the porous, amorphous pyrolyzed films (Fig. 1). A rigid gel network will not flow and densify prior to crystallization.

The dielectric constant of $BaTiO_3$ on (100) Si was measured to be ~40 at a frequency of 10 kHz. The properties of the film are degraded by the presence of the low-dielectric-constant, amorphous barium titanium silicate interfacial layer, because these layers are in series with the $BaTiO_3$ film. Attempts to crystallize the first layer prior to the deposition of subsequent layers resulted in the formation of polycrystalline $Ba_2TiSi_2O_8$. These interfacial reactions also have been detected in MOCVD-derived[1] and sputtered[5] $BaTiO_3$ films on silicon.

Preliminary dielectric measurements of films on platinum-coated silicon reveal that the intermediate carbonate phase, the porosity, and the fine grain size may have a detrimental effect on the properties. The dielectric constant of a $BaTiO_3$ film on platinum-coated silicon was measured to be ~200 at a frequency of 10 kHz; this is an order of magnitude lower than that

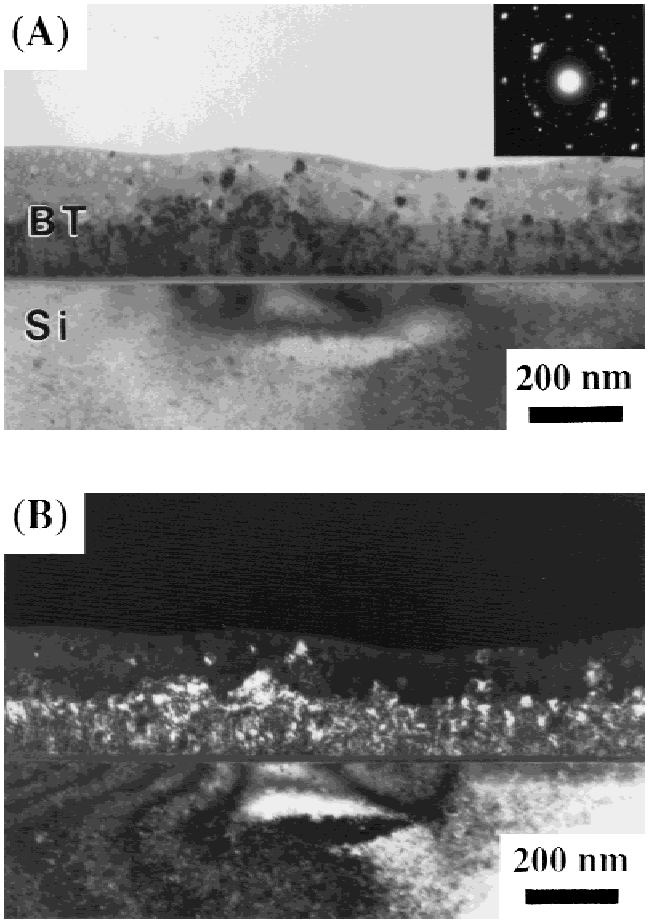

Fig. 13. Cross-sectional TEM micrographs ((A) bright field and (B) dark field, using the same reflections as in Fig. 10(B)) of sol–gel $BaTiO_3$ on $BaTiO_3$/(100) Si after *in-situ* TEM heating at 700°C for 5.5 h, showing some regions of oriented growth on the (100) $BaTiO_3$. The corresponding electron diffraction pattern is shown in the inset in Fig. 13(A).

of bulk $BaTiO_3$ at room temperature, although it is consistent with the results of others for measured dielectric constants of polycrystalline $BaTiO_3$ thin films.[15,26] With a nanocrystalline grain size, there is a high percentage of grain-boundary area that contributes to the properties. Porosity also will degrade the dielectric constant, as will any residual intermediate carbonate phase in the film.

It is clear than the minimization or elimination of the intermediate carbonate phase may lead to films with more-desirable electrical properties. It has been shown, for methoxyethoxide-derived $BaTiO_3$ powders, that high concentrations of water of hydrolysis that is added to the sol can prevent the formation of the intermediate phase by eliminating the carbon species through the release of carbon during drying.[14,34] In our studies of methoxypropoxide-derived powders, after adding 30 mol of water per mole of alkoxide ($h = 30$) to the sol, the dried powders crystallize directly to $BaTiO_3$ rather than the carbonate phase, which is similar to the results of Frey and Payne[34] on methoxyethoxide-derived powders. The problem with increasing the water of hydrolysis in sols for spin coating is that the water (even $h = 1$) causes precipitation in the sol, which makes it difficult to use the sol for spin coating. Recently, however, the group of Ono *et al.*[38] proposed a novel method to use precipitates in forming sols for coating, and their approach is being investigated to determine if it is applicable to this system.

V. Conclusions

Barium titanate ($BaTiO_3$) thin films that are prepared using a methoxypropoxide-based sol–gel method are polycrystalline and nanoporous, with a grain size of 20–60 nm. The development of this microstructure has been studied using *in-situ* TEM heating studies that have revealed that amorphous-gel films first crystallize to an intermediate phase at a temperature of ~600°C. It is proposed that this phase is $BaTiO_2CO_3$. This intermediate phase decomposes with a large weight loss at high temperatures and may contribute to the residual porosity in the films. Fine-grained $BaTiO_3$ seems to be nucleated by the decomposition of this intermediate phase. Nucleation in the bulk of the film is omnipresent. Even on lattice-matched substrates, such as MBE-grown $BaTiO_3$, randomly oriented crystallization of $BaTiO_3$ in the bulk occurs concurrently with oriented growth. It is possible to avoid the formation of this deleterious intermediate carbonate phase by the incorporation of a high concentration of water of hydrolysis in the sols, and although immediate precipitation occurs, methods to incorporate this approach into the formation of thin films are being studied.

Acknowledgments: The authors would like to thank Dr. R. A. McKee of Oak Ridge National Laboratory (Oak Ridge, TN) for providing the epitaxial $BaTiO_3$ substrates and Dr. John Vajo of Hughes Research Laboratories for the Auger studies.

References

[1]C. H. Lee and S. J. Park, ''Preparation of Ferroelectric $BaTiO_3$ Thin Films by Metal Organic Chemical Vapour Deposition,'' *J. Mater. Sci.: Mater. Electron.,* **1**, 219–24 (1990).

[2]B. S. Kwak, K. Zhang, E. P. Boyd, A. Erbil, and B. J. Wilkens, ''Metalorganic Chemical Vapor Deposition of $BaTiO_3$ Thin Films,'' *J. Appl. Phys.,* **69** [2] 767–72 (1991).

[3]V. P. Dravid, H. Zhang, L. A. Wills, and B. W. Wessels, ''On the Microstructure, Chemistry, and Dielectric Function of $BaTiO_3$ MOCVD Thin Films,'' *J. Mater. Res.,* **9** [2] 426–30 (1994).

[4]A. Yamanashi, K. Tanaka, T. Nagatomo, and O. Omoto, ''$BaTiO_3$ Films for Silicon-on-Insulator Structure,'' *Jpn. J. Appl. Phys., Part 1,* **32** [9B] 4179–81 (1993).

[5]Q. X. Jia, L. H. Chang, and W. A. Anderson, ''Interactions Between Ferroelectric $BaTiO_3$ and Si,'' *J. Electron. Mater.,* **23** [6] 551–56 (1994).

[6]S. Kim, S. Hishita, Y. M. Kang, and S. Baik, ''Structural Characterization of Epitaxial $BaTiO_3$ Thin Films Grown by Sputter Deposition on MgO(100),'' *J. Appl. Phys.,* **78** [9] 5604–608 (1995).

[7]K. Iijima, T. Terashima, K. Yamamoto, K. Hirata, and Y. Bando, ''Preparation of Ferroelectric $BaTiO_3$ Thin Films by Activated Reactive Evaporation,'' *Appl. Phys. Lett.,* **56** [6] 527–29 (1990).

[8]R. A. McKee, F. J. Walker, J. R. Conner, E. D. Specht, and D. E. Zelmon, ''Molecular Beam Epitaxy Growth of Epitaxial Barium Silicide, Barium Oxide, and Barium Titanate on Silicon,'' *Appl. Phys. Lett.,* **59** [7] 782–84 (1991).

[9]E. G. Jacobs, Y. G. Rho, R. F. Pinizzotto, S. R. Summerfelt, and B. E. Gnade, ''Effect of a Ge Barrier on the Microstructure of $BaTiO_3$ Deposited on Silicon by Pulsed Laser Ablation''; pp. 379–84 in *Laser Ablation in Materials Processing—Fundamentals and Applications,* Proceedings of the Materials Research Society Symposium, Vol. 285 (Boston, MA, December 1–4, 1992). Edited by B. Braren, J. J. Dubowski, and D. P. Norton. Materials Research Society, Pittsburgh, PA, 1993.

[10]M. G. Norton, K. P. B. Cracknell, and C. B. Carter, ''Pulsed-Laser Deposition of Barium Titanate Thin Films,'' *J. Am. Ceram. Soc.,* **75** [7] 1999–2002 (1992).

[11]K. Nashimoto, D. K. Fork, F. A. Ponce, and J. C. Tramontana, ''Epitaxial $BaTiO_3$/MgO Structure Grown on GaAs(100) by Pulsed Laser Deposition,'' *Jpn. J. Appl. Phys., Part 1,* **32** [9B] 4099–102 (1993).

[12]N. D. S. Mohallem and M. A. Aegerter, ''Sol–Gel Processed $BaTiO_3$''; pp. 515–18 in *Better Ceramics Through Chemistry III,* Proceedings of the Materials Research Society Symposium, Vol. 121 (Reno, NV, April 5–8, 1988). Edited by C. J. Brinker, D. E. Clark, and D. R. Ulrich. Materials Research Society, Pittsburgh, PA, 1988.

[13]K. A. Vorotilov, E. V. Orlova, V. I. Petrovsky, M. I. Yanovskaya, S. A. Ivanov, E. P. Turevskaya, and N. Y. Turova, ''$BaTiO_3$ Films on Silicon Wafers from Metal Alkoxides,'' *Ferroelectrics,* **123**, 261–71 (1991).

[14]J.-F. Campion, D. A. Payne, and H. K. Chae, ''Chemical Processing of Barium Titanate Powders and Thin Layer Dielectrics''; pp. 477–89 in Ceramic Transactions, Vol. 22, *Ceramic Powder Science IV.* Edited by D. E. Clark, F. D. Gac, and W. H. Sutton. American Ceramic Society, Westerville, OH, 1991.

[15]Z. Xu, H. K. Chae, M. H. Frey, and D. A. Payne, ''Chemical Processing and Properties of Nanocrystalline $BaTiO_3$''; pp. 339–44 in *Better Ceramics Through Chemistry V,* Proceedings of the Materials Research Society Symposium, Vol. 271 (San Francisco, CA, April 27–May 1, 1992). Edited by M. J. Hampden-Smith, W. G. Klemperer, and C. J. Brinker. Materials Research Society, Pittsburgh, PA, 1992.

[16]T. Hayashi, N. Ohji, K. Hirohara, T. Fukanaga, and H. Maiwa, ''Preparation and Properties of Ferroelectric $BaTiO_3$ Thin Films by Sol–Gel Process,'' *Jpn. J. Appl. Phys.,* **32**, 4092–94 (1993).

[17]M. I. Yanovskaya, N. M. Kotova, I. E. Obvintseva, E. P. Turevskaya, N. Y. Turova, K. A. Vorotilov, L. I. Solov'yova, and E. P. Kovsman, ''Preparation of Powders and Thin Films of Complex Oxides from Metal Alkoxides''; pp. 15–20

in *Better Ceramics Through Chemistry VI,* Proceedings of the Materials Research Society Symposium, Vol. 346 (San Francisco, CA, April 4–8, 1994). Edited by A. K. Cheetham, C. J. Brinker, M. L. Mecartney, and C. Sanchez. Materials Research Society, Pittsburgh, PA, 1994.

[18]Y. Xu, C. H. Cheng, and J. D. Mackenzie, ''Electrical Characterization of Polycrystalline and Amorphous Thin Films of $Pb(Zr_xTi_{1-x})O_3$ and $BaTiO_3$ Prepared by Sol–Gel Technique,'' *J. Non-Cryst. Solids,* **176**, 1–17 (1994).

[19]J. J. Xu, A. S. Shaikh, and R. W. Vest, ''High *K* $BaTiO_3$ Films from Metalloorganic Precursors,'' *IEEE Trans. Ultrason. Ferroelectr. Freq. Control,* **36** [3] 307–12 (1989).

[20]W. Ousi-Benomar, S. S. Xue, R. A. Lessard, A. Singh, Z. L. Wu, and P. K. Kuo, ''Structural and Optical Characterization of $BaTiO_3$ Thin Films Prepared by Metal-Organic Deposition from Barium 2-Ethylhexanoate and Titanium Dimethoxy Dineodecanoate,'' *J. Mater. Res.,* **9**, [4] 970–79 (1994).

[21]E. Ching-Prado, R. S. Katiyar, and J. J. Santiago-Aviles, ''Micro-Raman Study of $BaTiO_3$ Thin Films Prepared by the Metallo-Organic Decomposition Technique,'' *J. Raman Spectrosc.,* **25**, 215–19 (1994).

[22]H. Kawano, K. Morii, and Y. Nakayama, ''Microstructural and Dielectric Properties of $BaTiO_3$ Thin Films Prepared by Atom Beam Sputtering,'' *Mater. Lett.,* **12**, 252–56 (1991).

[23]S. Kumar and G. L. Messing, ''Metal Organic Resin Derived Barium Titanate: II, Kinetics of $BaTiO_3$ Formation,'' *J. Am. Ceram. Soc.,* **77** [11] 2940–48 (1994).

[24]M. C. Gust, L. A. Momoda, and M. L. Mecartney, ''Microstructure and Crystallization Behavior of Sol–Gel Prepared $BaTiO_3$ Thin Films''; see Ref. 17, pp. 649–53.

[25]T. Hayashi, N. Oji, and H. Maiwa, ''Film Thickness Dependence of Dielectric Properties of $BaTiO_3$ Thin Films Prepared by Sol–Gel Method,'' *Jpn. J. Appl. Phys.,* **33**, 5277–80 (1994).

[26]M. H. Frey and D. A. Payne, ''Nanocrystalline Barium Titanate: Evidence for the Absence of Ferroelectricity in Sol–Gel Derived Thin-Layer Capacitors,'' *Appl. Phys. Lett.,* **63** [20] 2753–55 (1993).

[27]G. Arlt, D. Hennings, and G. de With, ''Dielectric Properties of Fine-Grained Barium Titanate Ceramics,'' *J. Appl. Phys.,* **58** [4] 1619–25 (1985).

[28]M. C. Gust, L. A. Momoda, and M. L. Mecartney, ''Influence of Precursor Chemistry on the Microstructure and Crystallization of Barium Titanate Thin Films''; pp. 85–91 in Ceramic Transactions, Vol. 55, *Sol–Gel Science and Technology.* Edited by E. J. A. Pope, S. Sakka, and L. C. Klein. American Ceramic Society, Westerville, OH, 1995.

[29]A. S. Shaikh and G. M. Vest, ''Kinetics of $BaTiO_3$ and $PbTiO_3$ Formation from Metallo-Organic Precursors,'' *J. Am. Ceram. Soc.,* **69** [9] 682–88 (1986).

[30]A. Mosset, I. Gautier-Luneau, J. Galy, P. Strehlow, and H. Schmidt, ''Sol–Gel Processed $BaTiO_3$: Structural Evolution from the Gel to the Crystalline Powder,'' *J. Non-Cryst. Solids,* **100**, 339–44 (1988).

[31]H. S. G. Murthy, M. S. Rao, and T. R. N. Kutty, ''Thermal Decomposition of Titanyl Oxalates—I, Barium Titanyl Oxalate,'' *J. Inorg. Nucl. Chem.,* **37**, 891–98 (1975).

[32]D. Hennings and W. Mayr, ''Thermal Decomposition of (Ba,Ti) Citrates into Barium Titanate,'' *J. Solid State Chem.,* **26**, 329–38 (1978).

[33]S. Kumar, G. L. Messing, and W. B. White, ''Metal Organic Resin Derived Barium Titanate: I, Formation of Barium Titanium Oxycarbonate Intermediate,'' *J. Am. Ceram. Soc.,* **76** [3] 617–24 (1993).

[34]M. H. Frey and D. A. Payne, ''Synthesis and Processing of Barium Titanate Ceramics from Alkoxide Solutions and Monolithic Gels,'' *Chem. Mater.,* **7**, 123–29 (1995).

[35]Powder Diffraction File, Card No. 21-1276, Joint Committee on Powder Diffraction Standards (JCPDS), Swarthmore, PA (now International Centre for Diffraction Data (ICDD), Newtowne Square, PA), 1969.

[36]Powder Diffraction File, Card No. 20-143, Joint Committee on Powder Diffraction Standards (JCPDS), Swarthmore, PA (now International Centre for Diffraction Data (ICDD), Newtowne Square, PA), 1967.

[37]H. Oppolzer and H. Schmelz, ''Investigation of Twin Lamellae in $BaTiO_3$ Ceramics,'' *J. Am. Ceram. Soc.,* **66** [6] 444–46 (1983).

[38]S. Ono, T. Takeo, and S.-I. Hirano, ''Processing of Highly Oriented $LiNbO_3$ Films for Waveguides from Aqueous Solution,'' *J. Am. Ceram. Soc.,* **79** [5] 1343–50 (1996). □